Liquid Crystals
Publication details, including instructions for authors and subscription information:
http://www.informaworld.com/smpp/title~content=t713926090

Enhancement of the display parameters of 4'-pentyl-4-cyanobiphenyl due to the dispersion of functionalised gold nano particles

Abhay S. Pandey[a]; R. Dhar[a]; S. Kumar[b]; R. Dabrowski[c]
[a] Centre of Material Sciences, Institute of Interdisciplinary Studies, University of Allahabad, Allahabad, India [b] Raman Research Institute, Bangalore, India [c] Institute of Applied Sciences and Chemistry, Military University of Technology, Warsaw, Poland

Online publication date: 15 January 2011

To cite this Article Pandey, Abhay S. , Dhar, R. , Kumar, S. and Dabrowski, R.(2011) 'Enhancement of the display parameters of 4'-pentyl-4-cyanobiphenyl due to the dispersion of functionalised gold nano particles', Liquid Crystals, 38: 1, 115 — 120
To link to this Article: DOI: 10.1080/02678292.2010.530695
URL: http://dx.doi.org/10.1080/02678292.2010.530695

Liquid Crystals,
Vol. 38, No. 1, January 2011, 115–120

Taylor & Francis
Taylor & Francis Group

Enhancement of the display parameters of 4′-pentyl-4-cyanobiphenyl due to the dispersion of functionalised gold nano particles

Abhay S. Pandey[a], R. Dhar[a]*, S. Kumar[b] and R. Dabrowski[c]

[a]*Centre of Material Sciences, Institute of Interdisciplinary Studies, University of Allahabad, Allahabad, India;* [b]*Raman Research Institute, Bangalore, India;* [c]*Institute of Applied Sciences and Chemistry, Military University of Technology, Warsaw, Poland*

(*Received 20 September 2010; final version received 6 October 2010*)

We report electro-optical and dielectric studies of the gold nano particle (GNP) dispersed room-temperature liquid crystalline material 4′-pentyl-4-cyanobiphenyl (5CB) at a concentration of 0.1 wt%. Due to the dispersion of GNPs, the nematic to isotropic transition temperature is significantly increased. The threshold voltage required to switch molecules from the planar orientation (bright state) to the homeotropic (dark state) orientation is decreased. The dielectric parameters, namely, the longitudinal component of the dielectric permittivity and hence the dielectric anisotropy, are highly affected. The relaxation frequency corresponding to flip-flop motion of the 5CB molecules about their short axes has increased due to the presence of GNPs.

Keywords: nematic liquid crystal; electro-optical properties; gold nano particles; display parameters; transmission–voltage characteristic

1. Introduction

Study of the influence of nano systems on the properties of liquid crystals (LCs) has attracted considerable scientific interest since the beginning of the present decade [1]. One billionth of a metre, i.e. one nano metre, is considered to be a magical point on the dimensional scale. Nano-particle-doped LCs have been studied due to their gorgeous properties and prospective applications in the electronic industry by different groups around the world for viewing special aspects such as dielectric effects [2–12], electro-optics [2, 3, 5–11, 13–19], the memory effect [3, 14], photoluminescence [13] and fluorescence confocal polarising microscopy [20].

Nano particles share their intrinsic properties with LCs because of the mutual interactions at a molecular level due to the equality of the dimensions. The influence of nano particles on the liquid crystalline properties is generally achieved by adding a low concentration of nano particles into the LC matrix [2]. These dilute nano suspensions are stable due to the weak interactions of the particles at low concentrations. The nano particles are so small that they do not disturb the LC orientation and macroscopically identical structures are obtained, i.e. the suspensions appear similar to a pure LC with no readily apparent evidence of dissolved particles. At the same time the nano particles are sufficiently large to maintain the intrinsic properties of the materials from which they are made (e.g. the ferromagnetism or ferroelectricity) and they split these properties with the LC matrix due to anchoring with the LC. In most cases, nano particles reduce the threshold voltage (V_{th}) required to switch the molecules from a planar to a homeotropic configuration [2, 6, 7, 11, 14–19].

In the present work, we report a study on the changes that occur in the display parameters of a room temperature nematic material, namely, 4′-pentyl-4-cyanobiphenyl (5CB), due to the dispersion of functionalised gold nano particles (GNPs) of average size 2.4 nm. The nematic to isotropic phase transition temperature for pure 5CB is ∼35°C [21].

2. Experimental techniques

The gold clusters were prepared by a method described earlier [22, 23]. The method used furnishes 1.6 nm core diameter nano particles with an average composition of $Au_{140}[S(CH_2)_5CH_3]_{53}$ [22]. However, in the present study, the range of the synthesised nano particles was 1.6–3.1 nm with the majority of particles of size 2.4 nm as observed by transmission electron microscopy [24]. The distance between two GNPs was found to be about 4 nm. The LC–nano particle composite was prepared by mixing the required amount of GNPs and LC in anhydrous dichloromethane [23]. The solution was sonicated for 30 min at room temperature, followed by removal of solvent and drying under vacuum. The homogeneous nature of the nano composite was checked under a microscope and the nano composite was used as such for the present study.

For the study of the electro-optical (E-O) properties, polymer-coated and parallel-rubbed indium tin

*Corresponding author. Email: dr_ravindra_dhar@hotmail.com.

ISSN 0267-8292 print/ISSN 1366-5855 online

DOI: 10.1080/02678292.2010.530695
http://www.informaworld.com

oxide (ITO) coated glass plates with a pre-tilt angle of ~1–3° were used to prepare the cells with electrode spacing $d = 5$ μm. These cells were procured from Instec, USA. In such cells, the molecules are aligned parallel to the rubbing direction on the glass plates. The E-O characteristics, i.e. the transmission–voltage (T–V) curves were drawn by using polarised light microscopy coupled with a photo-detector unit from Instec. The photo-voltage (which is proportional to the intensity of the transmitted light) obtained from the photo-detector was recorded by using a six and half digit multimeter from Agilent (model-34410A). V_{th} was determined from the T–V curve.

In order to determine the other display parameters, dielectric data were acquired by using a Newton's Phase Sensitive Multimeter (model-1735) coupled with an Impedance Analysis Interface (IAI model-1257), in the frequency range 1 Hz to 35 MHz with both planar and homeotropic anchoring of the molecules. Instec cells are not appropriate for the measurement of dielectric parameters above 10 kHz due to the high resistance of the electrodes. Hence, we prepared our laboratory made cells from the ITO coated glass electrodes with a sheet resistance of ~10 Ω/□. Electrode surfaces were coated with polyamide nylon and then rubbed unidirectionally. Mylar spacers of thickness 10 μm were used to separate the electrodes. Using these cells, the transverse component of the relative dielectric permittivity ($\varepsilon'_{\perp}$) was determined. For the determination of the longitudinal component of the relative dielectric permittivity ($\varepsilon'_{\parallel}$), gold coated glass plates with another coating of lecithin were used to prepare the cells. In this case the thickness of the spacers was taken to be 40 μm. The temperature of the sample was controlled with the help of a hot-stage from Instec (model HS-1) having an accuracy of ±0.1°C. The dielectric permittivity (ε'), loss (ε'') and other parameters were obtained from the measured capacitance and conductance data of the cell filled with the samples as described earlier [25].

The measured dielectric spectra can be described with the help of the generalised Cole–Cole equation [26]

$$\varepsilon^* = \varepsilon' - j\varepsilon'' = \varepsilon'(\infty) + \frac{(\delta\varepsilon)}{1 + (jf\tau)^{(1-h)}} + \frac{A}{f^n} - j\frac{\sigma_{ion}}{2\pi\varepsilon_0 f^k} - jBf^m, \quad (1)$$

where $\delta\varepsilon$ ($= \varepsilon(0) - \varepsilon(\infty)$), τ and h are the dielectric strength, the relaxation time (inverse of the relaxation frequency) and the symmetric distribution parameter ($0 \leq h \leq 1$) of the relaxation mode, respectively. $\varepsilon(0)$ and $\varepsilon(\infty)$ are the low- and high-frequency limiting values of the relative dielectric permittivity. The third and fourth terms in Equation (1), represent the contribution of the electrode polarisation capacitance and ionic conductance at low frequencies where A and n are constants [27]. In the case of pure ohmic conductance, the constant k is found to be 1. The fifth imaginary term Bf^m is included in Equation (1) to partially account for the high-frequency parasitic effects [28, 29], B and m being constants as long as the correction is small. ε_0 (=8.85 pF m^{-1}) is the free space permittivity.

To explore the relaxation mode (wherever present) of the pure as well as dispersed systems, the experimentally observed dielectric permittivity and loss data were fitted with the real and imaginary parts of Equation (1), respectively. By the process of fitting, low- and high-frequency correction terms (parasitic effects) were discarded from the measured data to explore any existing relaxation phenomenon. Moreover, 10 kHz dielectric data were treated as the 'static' values, as they are often free from low- and high-frequency artefacts [27–30] and there is no dispersion mechanism up to this frequency. These data were used to determine the anisotropy of the relative dielectric permittivity $\Delta\varepsilon'(= \varepsilon'_{\parallel} - \varepsilon'_{\perp})$. Further details of the experimental technique including cell preparation are reported in earlier publications [29, 30].

3. Results and discussion

GNPs were dispersed in 5CB at a single concentration of 0.1 wt% because at higher concentrations they show a bundling effect whereas further low concentration dispersion is experimentally difficult to achieve with precision.

The optical texture of 5CB dispersed with 0.1 wt% of GNPs under the planar orientation is shown in Figure 1 and it confirms the uniform distribution of GNPs in the nematic matrix of 5CB. Various studies suggest that clearing, i.e. the nematic to isotropic transition temperature (T_{NI}), is increased by 3.3°C due to the dispersion of GNPs.

Figure 1 also shows T–V curves for pure and GNP dispersed 5CB samples at 23.0°C. At low voltages (less than V_{th}), molecules lie in the planar alignment and consequently a bright state is observed. When the applied voltage is increased above V_{th}, the molecules gradually turn to the homeotropic (with the molecular directors normal to the electrode surface) orientation and a dark state is observed. The voltage required to change the intensity from 90% to 10% of the maximum value is generally termed the switching voltage interval and this is the measure of the steepness of the T–V curve. Figure 1 shows that V_{th} has substantially reduced in the case of the GNP dispersed 5CB sample

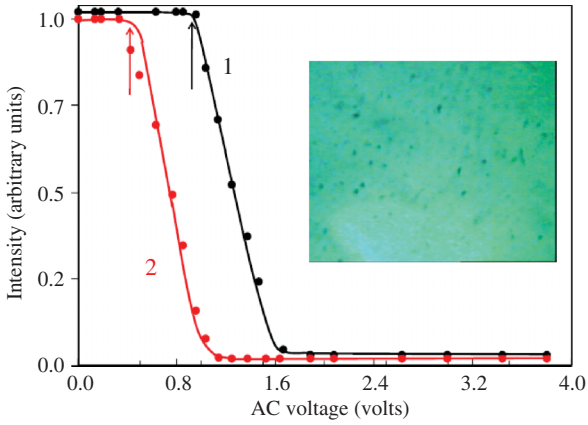

Figure 1. Electro-optical response to the applied alternating voltage (1 kHz) for (1) the pure 5CB sample and (2) the GNPs dispersed in 5CB. Vertical upward arrows represent the threshold voltages. The microphotograph in the inset represents the bright state of the cell with the GNPs dispersed in 5CB (colour version online).

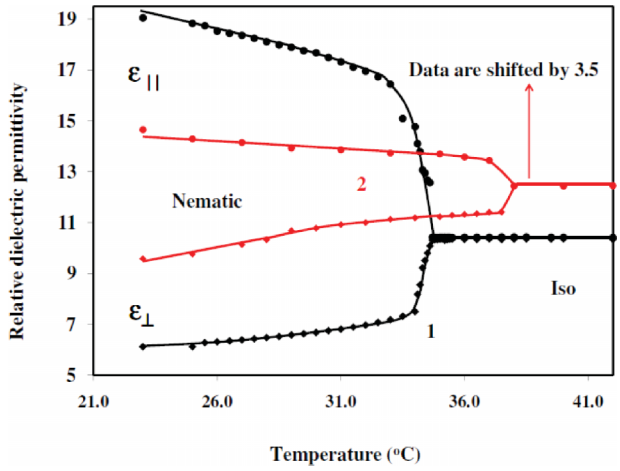

Figure 2. Temperature dependence of the longitudinal ($\varepsilon'_{\parallel}$) and transverse ($\varepsilon'_{\perp}$) components of the static relative dielectric permittivity (10 kHz) in the nematic and isotropic phases of (1) the pure 5CB and (2) the GNPs dispersed in 5CB. The second set of data are shifted upwards by 3.5 to increase the visibility of the data points (colour version online).

which is beneficial from an application point of view. The threshold voltage is governed by the equation

$$V_{\text{th}} = \pi \left(\frac{K_{11}}{\varepsilon_0 \Delta\varepsilon'} \right)^{\frac{1}{2}}, \qquad (2)$$

where K_{11} is the splay elastic constant.

In order to find the other parameters of Equation (2), we carried out dielectric measurements on the samples as described earlier. Variations of $\varepsilon'_{\parallel}$ and $\varepsilon'_{\perp}$ (and hence $\Delta\varepsilon' = \varepsilon'_{\parallel} - \varepsilon'_{\perp}$) with temperature are shown in Figure 2 for the pure sample as well as the GNP dispersed sample. Figure 2 shows that although $\varepsilon'_{\perp}$ remains almost unchanged, $\varepsilon'_{\parallel}$ has drastically decreased in the case of the GNP dispersed sample. Thus $\Delta\varepsilon'$ of the GNP dispersed sample has decreased significantly. Despite the decrease of $\Delta\varepsilon'$, V_{th} has decreased (see Figure 1) which suggests that K_{11} is also decreasing (Equation (2)) due to the dispersion of GNPs. The decrease of K_{11} may increase the switch-off time ($\tau_{\text{off}} = \gamma d^2/\pi K_{11}$, with γ being the dynamic viscosity of the material) and hence slow down the switching speed in the case of the GNP dispersed sample. Figure 2 also confirms the increase of T_{NI} for the GNP dispersed sample as compared to that of the pure sample. Various parameters obtained from Figures 1 and 2 are also summarised in Table 1 for clarity. It is important to mention here that, for the low optical anisotropy materials, low values of $\Delta\varepsilon'/\varepsilon'_{\perp}$ (<1) are desirable for improving the steepness of the T–V curve. In the case of the pure 5CB sample (e.g. at 23.0°C), $\varepsilon'_{\parallel} = 19.05$ and $\varepsilon'_{\perp} = 6.12$, i.e. $\Delta\epsilon' = 12.93$ and therefore $\Delta\varepsilon'/\varepsilon'_{\perp}$ is 2.11. For the GNP dispersed sample (at 23.0°C), $\varepsilon'_{\parallel} = 11.15$ and $\varepsilon'_{\perp} = 6.08$, i.e. $\Delta\varepsilon' = 5.07$ and $\Delta\varepsilon'/\varepsilon'_{\perp}$ is 0.83. This suggests that $\Delta\varepsilon'/\varepsilon'_{\perp}$ is significantly decreasing due to the dispersion of GNPs. This effect can be utilised in appropriate material (i.e. materials with low optical anisotropy) for the tuning of the steepness of the T–V curves.

It is important to mention here that there are several publications where an increase of T_{NI} has been reported due to the dispersion of ferroelectric nano particles and possible theoretical explanations are also reported [31, 32]. However, to the best of our knowledge there is no report indicating an increase of T_{NI} due to the dispersion of GNPs. Prasad *et al.* studied the effect of GNP dispersion in 5CB but they found the opposite effect on T_{NI}, i.e. it decreases due to the presence of GNPs [12]. Further, they observed almost no change in the dielectric parameters due to the dispersion of GNPs. In the present work, we have taken the size of GNPs to be ~2.4 nm [24] in contrast to the size of 15–20 nm in earlier studies in order to make it comparable with the size of the molecules of 5CB. It is important to mention that in the present case nano particles are functionalised with almost 10 alkyl chains (five on each side of the GNP) [23]. This may increase the effective chain length of the molecules and be responsible for the increase in the nematic to isotropic transition temperature of the LC–GNP composite.

Now we come to the explanation of the change in various parameters. The static dielectric parameters of the nematic phase are governed by the Maier and Meier theory [33]. The longitudinal ($\varepsilon'_{\parallel}$) and transverse ($\varepsilon'_{\perp}$) components of the dielectric permittivity are given as

Table 1. The nematic to isotropic transition temperature (T_{NI}), the threshold voltage (V_{th}), the dielectric anisotropy ($\Delta\varepsilon'_{\perp}$), the ratio of the dielectric anisotropy to the transverse component of the dielectric permittivity ($\Delta\varepsilon'/\varepsilon'_{\perp}$), the relaxation frequency (f_r) and the activation energy (E_a) for the nematic phase corresponding to flip-flop motion of molecules about their short axes (at 23.0°C).

Sample	T_{NI} (°C)	V_{th} (V)	$\Delta\varepsilon'_{\perp}$	$\Delta\varepsilon'/\varepsilon'_{\perp}$	f_r (MHz)	E_a (kJ/mol)
Pure 5CB	34.7	0.85	12.93	2.11	3.8	81
GNP dispersed 5CB	38.0	0.33	5.07	0.83	5.7	74

$$\varepsilon'_{\parallel} = 1 + \frac{NHF}{\varepsilon_0}\left\{\alpha_{av} + \frac{2}{3}S\Delta\alpha + Fg_{\parallel}\frac{\mu^2}{3kT}\left[1 - \left(1 - 3\cos^2\beta\right)S\right]\right\}, \quad (3)$$

$$\varepsilon'_{\perp} = 1 + \frac{NHF}{\varepsilon_0}\left\{\alpha_{av} - \frac{1}{3}S\Delta\alpha + Fg_{\perp}\frac{\mu^2}{3kT}\left[1 + \left(\frac{1}{2} - 3\cos^2\beta\right)S\right]\right\}. \quad (4)$$

Equations (3) and (4) yield the dielectric anisotropy

$$\Delta\varepsilon' = \frac{NHF}{\varepsilon_0}\left[\Delta\alpha - \frac{F}{2kT}\mu^2(1 - 3\cos^2\beta)\right]S. \quad (5)$$

Further, Equations (3) and (4) reduce to give the dielectric permittivity of the isotropic phase (ε'_i),

$$\varepsilon'_i = 1 + \frac{NHF}{\varepsilon_0}\left\{\alpha_{av} + F\frac{\mu^2}{3kT}\right\}, \quad (6)$$

where N is the number density of molecules and S is the order parameter. $\Delta\alpha$ is the anisotropy of the polarisability, α_{av} the average polarisability, μ the resultant dipole moment of the molecule and β the angle between the dipole moment and the long axis of the molecule. F is the feedback factor and $H = 3\varepsilon(0)/(2\varepsilon(0)+1)$. According to Maier and Meier theory, the parameters mentioned above significantly depend upon N, S, μ and β. Here, it is possible that due to the dispersion of GNPs, a decrease of the number density of 5CB molecules may be the cause of the decrease of $\varepsilon'_{\parallel}$, ε'_i and $\Delta\varepsilon'$. However, it does not appear the appropriate reason because firstly a change in N due to GNP dispersion is very small and cannot account for the large change observed in the above parameters. Secondly, a change has not been observed in $\varepsilon'_{\perp}$. Prasad *et al.* have also not observed any significant change in these parameters for the GNP concentration as high as 5%. The same factors rule out any possibility for a decrease in S. Similarly, we do not expect a change in β as well. However, it is most reasonable to accept that the presence of functionalised GNPs decreases the longitudinal component of the effective dipole moment by producing a strong dipole moment anti-parallel to the longitudinal component of the dipole moment of the 5CB molecules but without affecting the transverse component of the dipole moment of the 5CB molecules. Development of such an anti-parallel dipole moment due the presence of GNPs is responsible for the stabilisation of the nematic phase thereby increasing T_{NI} as proposed by Lena and Jonathan [32]. Here it is important to mention that in the work of Lena and Jonathan [32] it has been proposed that, under the strong electric field of ferroelectric nano particles, LC molecules align anti-parallel. However, in the present case, it is suggestive that under the influence of the electric field of the longitudinal component of the dipole moment of 5CB molecules, functionalised GNPs develop a strong anti-parallel dipole moment due to the displacement of conduction electron charge clouds relative to the nuclei as in the case of localised surface plasmons [34, 35]. One should keep in mind that, in the case of 5CB molecules, the longitudinal component of the dipole moment is very much larger than the transverse component. However, such an effect can be observed only if the size of the GNPs is comparable with the molecular size of 5CB as in the present case.

The presence of spherically symmetric GNPs in between the anisotropic 5CB molecules is responsible for the decrease of K_{11} as observed earlier in a single wall carbon nano tube (SWCNT) doped nematic system [11].

Although in the case of planar oriented molecules we have not observed any relaxation mode in the pure as well as in the GNP dispersed samples up to 10 MHz, in the case of homeotropic aligned molecules we have detected a relaxation mode in the MHz frequency region (see Figure 3), which corresponds to flip-flop motion of the molecules about their short axes. However, it has been observed that, in the case of GNP dispersed samples, the relaxation frequencies go up when compared to the pure sample (see Table 1). This happens because of the increase in the

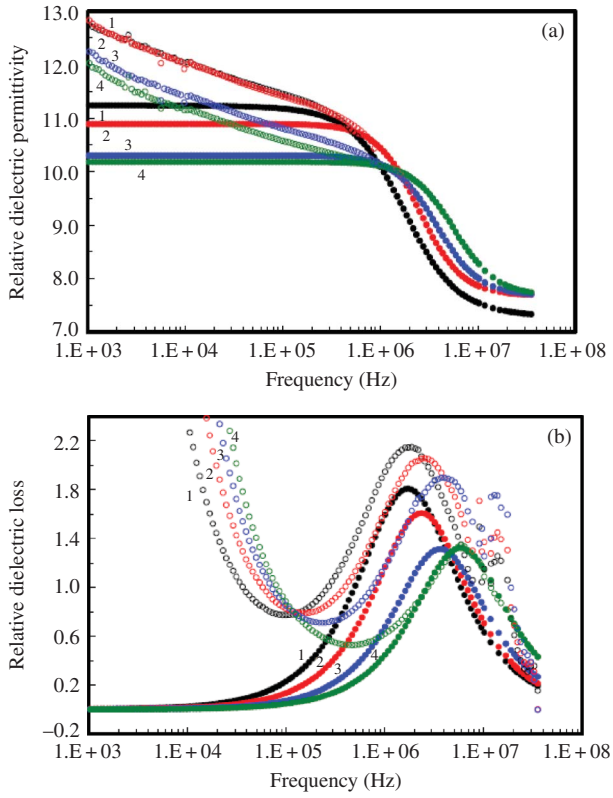

Figure 3. Frequency dependence of (a) the longitudinal component of the relative dielectric permittivity ($\varepsilon'_{\parallel}$) and (b) the corresponding loss in the homeotropic aligned samples at different temperatures: (1) 11.0°C, (2) 15.0°C, (3) 19.0°C and (4) 23.0°C for GNPs dispersed in 5CB. Hollow circles represent the raw experimental data, while filled circles represent the data extracted by the process of fitting of Equation (1). Similar plots but with low relaxation frequencies have been observed for pure 5CB (colour version online).

availability of the volume for molecular motion due to the presence of spherical GNPs [36]. GNPs work as spacers without occupying much space as compared to 5CB molecules. The relaxation frequencies (f_r) follow the Arrhenius equation,

$$f_r = A \exp\left(\frac{-E_a}{N_A k T}\right), \tag{7}$$

where N_A is the Avogadro number, k is the Boltzmann constant and E_a is the activation energy corresponding to the flip-flop motion of the molecules about their short axes. The slopes of the plots of log (f_r) versus the inverse of the temperature were obtained by the method of least-squares fit. With the help of the slopes of the straight lines, the activation energies (E_a) were obtained for the pure and dispersed systems (see Table 1). It can be observed that E_a decreases due

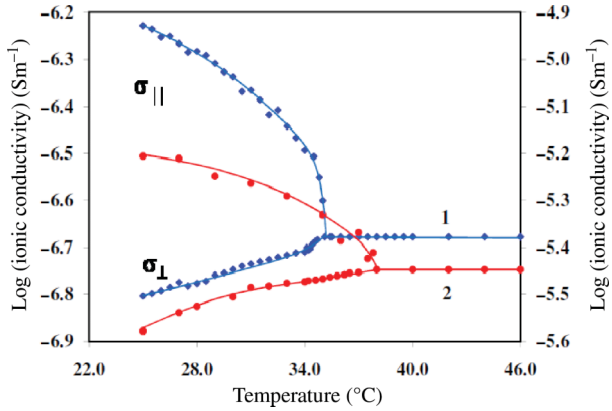

Figure 4. The temperature dependence of the ionic conductivity in the directions parallel and perpendicular to the director of (1) the pure 5CB sample on the primary axis and (2) the GNPs dispersed in 5CB on the secondary axis (colour version online).

to the presence of GNPs in the sample. This also suggests that the presence of GNPs facilitates the flip-flop motion of the molecules thereby decreasing E_a.

The temperature dependences of the ionic conductivity of the pure as well as the composite of GNPs with 5CB, both parallel and perpendicular to the molecular axes, are shown in Figure 4. It is found that the ionic conductivity of the GNP dispersed 5CB increases approximately seven to eight times compared to that of the pure sample. The electrical conductivity anisotropy defined as $\Delta\sigma = \sigma_{||} - \sigma_{\perp}$ is also apparent in Figure 4. Prasad *et al.* also found that the inclusion of GNP increases the electrical conductivity by more than two orders of magnitude for the 5% concentration of GNPs in the LC system. The inclusion of GNPs in 5CB affected both the components of the electrical conductivity. They suggested that the GNPs behave like an ionic additive to the LC system. However, another reason may be the availability of extra space in the sample due to the presence of spherical GNPs in the closely packed 5CB molecules. The availability of the additional space will facilitate the motion of ions in the sample.

4. Conclusions

It has been observed that the presence of functionalised GNPs in the nematic matrix of 5CB increases the nematic to isotropic transition temperature significantly, and decreases the threshold voltage required for switching of molecules from the planar (bright state) to the homeotropic (dark state) configuration and the ratio of the dielectric anisotropy to the transverse component of the permittivity. The presence of functionalised GNPs also decreases the effective longitudinal component of the dipole moment of the system

due to the formation of anti-parallel dipoles thereby increasing the stability of the nematic phase and causing a consequent increase in the nematic to isotropic transition temperature.

Acknowledgements

The authors thank the Department of Science and Technology (DST), New Delhi for financial assistance under Project number SR/S2/CMP-12/2006. ASP thanks DST for a Senior Research fellowship under the project.

References

[1] Stark, H. *Phys. Rep.* **2001**, *351*, 387–474.
[2] Reznikov, Y.; Buchnev, O.; Tereshchenko, O.; Reshetnyak, V.; Glushchenko, A.; West, J. *Appl. Phys. Lett.* **2003**, *82*, 1917–1919.
[3] Prakash, J.; Choudhary, A.; Kumar, A.; Mehta, D.S.; Biradar, A.M. *Appl. Phys. Lett.* **2008**, *93*, 112904-1-3.
[4] Ouskova, E.; Buchnev, O.; Reshetnyak, V.; Reznikov, Y.; Kresse, H. *Liq. Cryst.* **2003**, *30*, 1235–1239.
[5] Neeraj; Raina, K.K. *Phase trans.* **2010**, *83*, 615–626.
[6] Shiraishi, Y.; Toshima, N.; Maeda, K.; Yoshikawa, H.; Xu, J.; Kobayashi, S. *Appl. Phys. Lett.* **2002**, *81*, 2845-1-3.
[7] Haraguchi, F.; Inoue, K.; Toshima, N.; Kobayashi, S.; Takotoh, K. *Jpn. J. Appl. Phys.* **2007**, *34*, L796–L797.
[8] Mikulko, A.; Arora, P.; Glushchenko, A.; Lapanik, A.; Haase, W. *Euro Phys Lett* **2009**, *87*, 27009-1-4.
[9] Dhar, R.; Paul, S.N.; Sharma, S.; Dabrowski, R. *XVIII Conf. on Liq. Cryst. (Chemistry, Physics & Applications)*, Augustow, Poland, 14–18 September, 2009.
[10] Paul, S.N.; Dhar, R.; Verma, R.; Sharma, S.; Dabrowski, R. *23rd Int. Liq. Cryst. Conf*., Krakow, Poland, 11–16 July, 2010.
[11] Dhar, R.; Pandey, A.S.; Pandey, M.B.; Kumar, S.; Dabrowski, R. *App. Phys. Exp.* **2008**, *1*, 121501-1-3.
[12] Prasad, S.K.; Sandhya, K.L.; Geetha, G.N.; Uma, S.H.; Yelamaggad, C.V.; Sampath, S. *Liq. Cryst.* **2006**, *33*, 1121–1125.
[13] Kumar, A.; Prakash, J.; Mehta, D.S.; Biradar, A.M.; Haase, W. *Appl. Phys. Lett.* **2009**, *95,* 023117-1-3.
[14] Kaur, S.; Singh, S.P.; Biradar, A.M.; Choudhary, A.; Sreenivas, K. *Appl. Phys. Lett.* **2007**, *91*, 023120-1-3.
[15] Qi, H.; Kinkead, B.; Hegmann, T. *Adv. Funct. Mater.* **2008**, *18*, 212–221.
[16] Kinkead, B.; Hegmann, T. *J. Mater. Chem.* **2010**, *20*, 448–458.
[17] Hinojosa, A.; Sharma, S.C. *Appl. Phys. Lett.* **2010**, *97*, 081114-1-3.
[18] Buchnev, O.; Dyadyusha, A.; Kachmarek, M.; Reshetnyak, V.; Reznikov, Y. *J. Opt. Soc. Am. B* **2007**, *24*, 1512–1516.
[19] Cheon, C.I.; Li, L.; Glushchenko, A.; West, J.L.; Reznikov, Y.; Kim, J.S.; Kim, D.H. *SID Int. Symp. Dig. Tech. Pap.* **2005**, *36*, 1471–1473.
[20] Urbanski, M.; Kinkead, B.; Hegmann, T; Kitzerow, H.S. *Liq. Cryst.* **2010**, *37*, 1151–1156.
[21] Dunmur, D.A.; Manterfield, M.R.; Miller, W.H.; Dunleavy, J.K. *Mol. Cryst. Liq. Cryst.* **1978**, *45*, 127–144.
[22] Song, Y.; Huang, T.; Murray, R.W. *J. Am. Chem. Soc.* **2003**, *125*, 11694–11701.
[23] Kumar, S.; Lakshminarayanan, V. *Chem. Commun.* **2004**, 1600–1601.
[24] Kumar, S.; Pal, S.K.; Kumar, P.S.; Lakshminarayanan, V. *Soft Matter* **2007**, *3*, 896–900.
[25] Dhar, R.; Verma, R.; Rath, M.C.; Sarkar, S.K.; Wadhawan, V.K.; Dabrowski, R.; Tykarska, M. *Appl. Phys. Lett.* **2008**, *92*, 014108-1-3.
[26] Cole, K.S.; Cole, R.H. *J. Chem. Phys.* **1941**, *9*, 341–351.
[27] Srivastava, S.L.; Dhar, R. *Indian. J. Pure Appl. Phys.* **1991**, *29*, 745–751.
[28] Srivastava, S.L. *Proc. Natl. Acad. Sci. India* **1993**, *63*, 311–324.
[29] Dhar, R. *Indian J. Pure Appl. Phys.* **2004**, *42*, 56–61.
[30] Pandey, M.B.; Dhar, R.; Agrawal, V.K.; Dabrowski, R.; Tykarska, M. *Liq. Cryst.* **2004**, *31*, 973–987.
[31] Fenghua, L.; Oleksandr, B.; Chae, I.C.; Anatoliy, G.; Victor, R.; Yuri, R.; Timothy, J.S.; John, L.W. *Phys. Rev. Lett.* **2006**, *97*, 147801-1-4; Fenghua, L.; Oleksandr, B.; Chae, I.C.; Anatoliy, G.; Victor, R.; Yuri, R.; Timothy, J.S.; John, L.W. *Phys. Rev. Lett.* **2007,** *99*, 219901(E).
[32] Lena, M.L.; Jonathan, V.S. *Phys. Rev. Lett.* **2009**, *102*, 197802-1-4.
[33] Maier, W.; Meier, G. *Z. Naturforsch* **1961**, *16A*, 262–267.
[34] Hutter, E.; Fendler, J.H. *Adv. Mater. (Weinheim, Ger.)* **2004**, *16*, 1685–1705.
[35] Kelly, K.L.; Coronado, E.; Zhao, L.L.; Schatz, G.C. *J. Phys. Chem. B* **2003**, *107*, 668–677.
[36] Edwards, D.M.F.; Madden, P.A. *Mol. Phys.* **1983**, *48*, 471–493.